Appl Phys B (2011) 104:591–595
DOI 10.1007/s00340-011-4386-6

Applied Physics B
Lasers and Optics

Millijoule intracavity OPO driven by a passively Q-switched Nd:YVO_4 laser with AlGaInAs quantum-well saturable absorber

Y.P. Huang · P.Y. Chiang · Y.F. Chen · K.F. Huang

Received: 29 October 2010 / Revised version: 5 January 2011 / Published online: 5 February 2011

Abstract We originally demonstrate the use of an AlGaInAs periodic quantum-well absorber to achieve a quasi-continuous-wave (QCW) diode-pumped passively Q-switched Nd:YVO_4 laser with an intracavity optical parametric oscillator (OPO). With a diode-pumping energy of 35 mJ, the output pulse energy and the pulse width at 1573 nm are found to be 1.58 mJ and 26 ns, respectively. The pulse repetition rate can be up to 100 Hz with the overall OPO beam quality M^2 factor to be better than 1.5.

1 Introduction

Low-eye-hazard lasers are inevitable in many applications such as laser radar, range finder, remote sensing, and target designation [1, 2]. High-repetition-rate eye-safe laser with single pulse energy in the millijoule (mJ) range is desired in LIDAR applications because of its long-range performance and high-speed data collection. One promising method for efficient eye-safe laser sources is based on optical parametric oscillators intracavity pumped by the Q-switched neodymium lasers emitting around 1 μm [3, 4]. Recently, eye-safe intracavity OPOs driven by quasi-cw (QCW) diode-pumped passively Q-switched Nd:YAG lasers have been demonstrated to generate mJ pulses [5–7]. Nevertheless, the highest repetition rate of mJ eye-safe intracavity OPOs achieved with QCW diode-pumped passively Q-switched Nd:YAG lasers are 40 Hz [7]. To achieve the high-repetition-rate eye-safe OPO in a QCW diode-pumped system, Nd-doped vanadate crystals with short fluorescence lifetime is required [8, 9]. Moreover, compared with Nd:YAG crystals, Nd-doped vanadate crystals have a higher absorption cross section, wider absorption bandwidth, and linear polarized output. As a result, Nd-doped vanadate crystals are a promising candidate for a high-repetition-rate mJ-level laser system. Even so, mJ-level eye-safe pulses based on the Nd-doped vanadate laser systems have not been realized as yet.

Diode-pumped passively Q-switched Nd:YVO_4/Cr^{4+}:YAG/KTP eye-safe lasers have been demonstrated [10–13]. However, Cr^{4+}:YAG crystals are usually not appropriate to directly serve as saturable absorbers for Nd:YVO_4 crystal lasers because their absorption cross sections are not high enough for the good Q-switched criterion [14]. To the best of our knowledge, the single pulse energies generated from Nd:YVO_4/Cr^{4+}:YAG based intracavity OPOs at 1.57 μm were several tens of μJ [10–13]. Recently, an AlGaInAs semiconductor material with a periodic quantum-well (QW) structure grown on a Fe-doped InP structure has been directly used as a saturable absorber in a CW and a QCW diode-pumped Nd:YVO_4 lasers [15, 16]. The excellent Q-switching efficiency indicates that AlGaInAs QW absorbers have a potential to pump an intracavity OPO.

In this work, we demonstrate for the first time the use of an AlGaInAs periodic QW device as a saturable absorber to realize a QCW diode-pumped passively Q-switched Nd:YVO_4 laser with an intracavity OPO. We employ a flat-flat cavity with an internal convex lens to achieve the mode-size matching and an efficient OPO conversion. With the optimum output reflectivity and at a pump energy of 35 mJ, the output pulse energy and the pulse width at 1573 nm are found to be 1.58 mJ pulse and 26 ns, respectively. Experimental results reveal that the pulse repetition rate can be up to 100 Hz with the overall OPO beam quality M^2 factor to be better than 1.5.

Y.P. Huang · P.Y. Chiang · Y.F. Chen (✉) · K.F. Huang
Department of Electrophysics, National Chiao Tung University, 1001 Ta Hsueh Road, Hsinchu 30050, Taiwan
e-mail: yfchen@cc.nctu.edu.tw

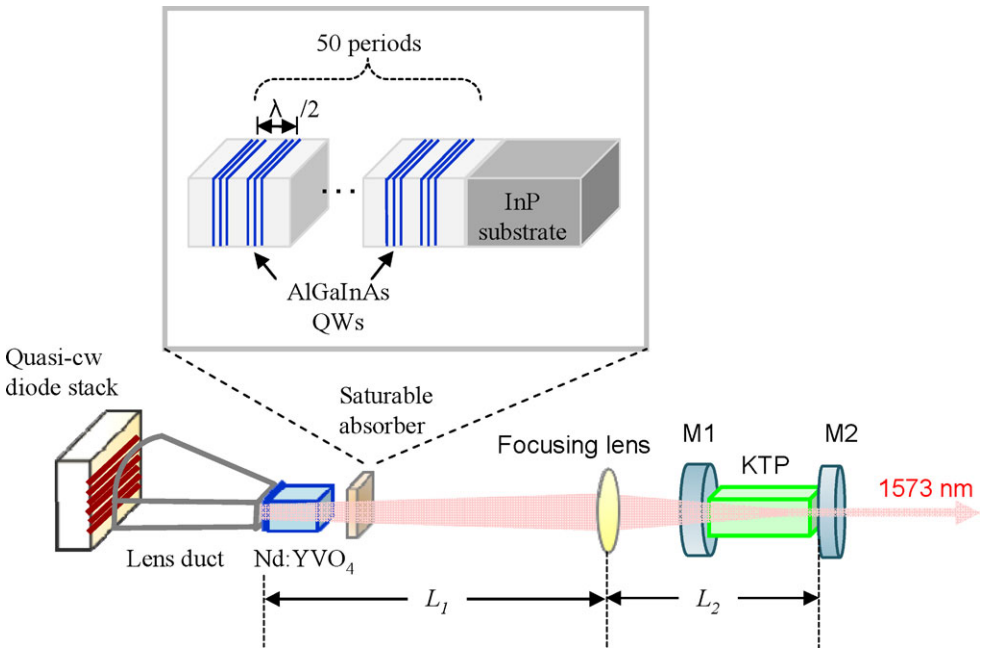

Fig. 1 Schematic diagram of the experiment setup for an intracavity OPO pumped by a QCW diode-pumped passively Q-switched Nd:YVO_4 laser with AlGaInAs/InP QWs used as a saturable absorber

2 Experimental setup

Figure 1 depicts the experiment setup for an intracavity OPO pumped by a QCW diode-pumped passively Q-switched Nd:YVO_4 laser with AlGaInAs/InP QWs used as a saturable absorber. The OPO cavity was formed by two flat mirrors. The first mirror M1 had a dichroic coating with highly reflective at 1573 nm ($R > 99.8\%$) and highly transmittance at 1064 nm ($T > 95\%$). The output coupler M^2 had a dichroic coating with highly reflective at 1064 nm ($R > 99.8\%$) and partially reflective at 1573 nm. A KTP crystal was used to be the nonlinear crystal of the OPO. The KTP crystal, $5 \times 5 \times 30$ mm^3, was employed in a type II noncritical phase-matching configuration along the x axis ($\theta = 90°$, and $\phi = 0°$) to have both a maximum effective nonlinear coefficient and no walk off between the pump, signal, and idler beams.

The pump source was a QCW high-power diode stack (Coherent G-stack package, Santa Clara, CA USA) which consisted of six 10-mm-long diode bars with a maximum output power of 120 W per bar at the central wavelength of 808 nm. The diode stack was constructed with 400 μm spacing between the diode bars so the whole emission area was approximately 10×2.4 mm^2. The full divergence angles in the fast and slow axes are approximately 35° and 10°, respectively. The pump duration of QCW laser diode stack was 100 μs to match the upper-level lifetime of Nd:YVO_4 laser crystal. A lens duct, which was fabricated from BK7 glass, was utilized to efficiently deliver the pump radiation to the laser crystal [17–19]. Compared with ordinary coupling methods, the lens duct has the advantages of simple structure, optical coupling efficiency, and spatial homogeneity of the pump intensity distribution. In this experiment, the lens duct dimensions are as follows: radius of curvature of the input surface 10 mm, width of the input surface 12 mm, length of the duct 29 mm, and output aperture 3.8 mm × 3.8 mm. The coupling efficiency of the lens duct was experimentally measured to be approximately 80%. The spatial distribution of the pumping beam after the lens duct was recorded with an infrared CCD. The pumping beam diameter was found to be 2.5 mm. The full divergence angles of the exit aperture of the lens duct in the fast and slow axes were approximately 40° and 20°, respectively. The active medium was an a-cut 0.5 at.% Nd^{3+}, 7-mm long Nd:YVO_4 crystal. The incident surface of the laser crystal was coated to be highly reflective at 1064 nm and 1573 nm ($R > 99.8\%$) and highly transmitted at 808 nm ($T > 90\%$) as the front mirror. The other surface of the laser crystal was coated with antireflection at 1064 nm and 1573 nm ($R < 0.2\%$). The laser crystal and OPO crystal were wrapped with indium foil and mounted in copper blocks.

The saturable absorber is an AlGaInAs QW/barrier structure grown on a Fe-doped InP structure by metalorganic chemical-vapor deposition. The saturable absorber consists of 50 groups of three QWs, spaced at half-wavelength intervals by InAlAs barrier layers with the band-gap wavelength around 806 nm and with the luminescence wavelength to be near 1064 nm. An InP window layer was deposited on the QW/barrier structure to avoid surface recombination and oxidation. The backside of the substrate was mechanically polished after growth. The both sides of the semiconductor saturable absorber were antireflection coated to reduce back reflections and the couple-cavity effects. The initial transmission of the absorber at 1064 nm was measured to be ap-

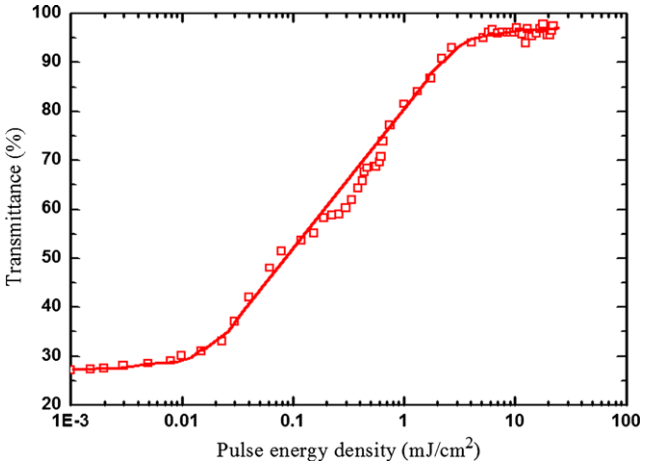

Fig. 2 Measured result for the transmittance of AlGaInAs material as a function of the incident pulse energy density at 1064 nm

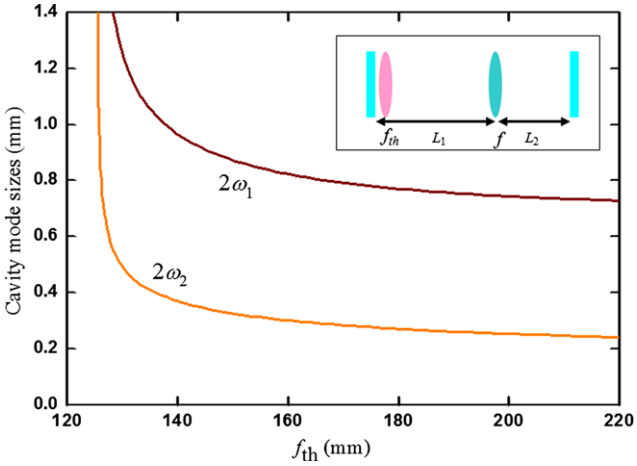

Fig. 3 Calculated results for the dependence of the cavity mode sizes on the focal length of the thermal lens. Inset: cavity configuration for numerical calculations

proximately 22%. A 1064-nm Q-switched laser with a pulse duration of 4 ns was used as the excitation source to measure the characteristic of the AlGaInAs QW saturable absorber. The transmittance of AlGaInAs material as a function of the incident pulse energy density at 1064 nm is shown in Fig. 2. The finial transmission of the absorber was found to be 95%, and the saturation energy density of the saturable absorber was estimated to be in the range of 1 mJ/cm^2. Employing the Frantz–Nodvik equation [20] to the saturation curve, the absorption cross section was calculated to be 9×10^{-16} cm^2.

3 Cavity analysis

As shown in Fig. 1, we employ a flat-flat resonator with an internal convex lens to form a passively Q-switched laser and to pump the intracavity OPO, where L_1 is the distance between the front mirror and the convex lens, L_2 is the distance between the convex lens and the output coupler M^2. In the past years, the three-element resonator, consisting of a flat rear mirror, a convex lens and a flat output coupler, has been identified to be an effective method for realizing the Kerr-lens mode-locked laser [21, 22]. The linear three-element resonator is beneficial for easy assembly, mode-matching design, and insensitivity to misalignment. Therefore, we employ the linear three-element resonator to design an intracavity OPO driven by a passively Q-switched Nd:YVO_4 laser with AlGaInAs QWs as a saturable absorber.

The KTP crystal was designed to be close to the output coupler. The mode diameters at the front mirror $2\omega_1$ and at the output coupler $2\omega_2$ are designed to be 0.85 and 0.28 mm, respectively, for achieving an efficient OPO conversion. Consequently, the required mode-size ratio ω_1/ω_2 is approximately 3. The focal length of the convex lens is chosen to be $f = 100$ mm. With the ABCD-matrix method, the appropriate values of L_1 and L_2 were found to approximately 351 mm and 124 mm, respectively. Figure 3 shows the calculated results for the mode diameters $2\omega_1$ and $2\omega_2$ as functions of the focal length of the thermal lensing effect. It can be seen that as long as the effective focal power of the thermal lens in the laser crystal is smaller than $2(L_1 - f)^{-1}$, the mode sizes can excellently meet the demands of the mode sizes.

4 Experimental results and discussion

First of all, the free-running operation without saturable absorber and KTP crystal was performed. A flat output coupler with 90% reflectivity at 1064 nm was used. Figure 4 plots the experimental results of the output energy with respect to the diode pump energy in the free-running operation. With a diode pumping energy of 37 mJ, the output energy at 1064 nm is approximately 15 mJ. The pump energy is defined as the energy delivered at the output of the lens duct.

We next confirmed the performance of the passively Q-switched Nd:YVO_4 laser with the AlGaInAs QWs before the intracavity OPO experiment. The optimum Q-switched performance at 1064 nm provides the baseline for evaluating the conversion efficiency of the intracavity OPO. A flat output coupler was utilized, and the optimum reflectivity of the output coupler was found to be approximately 50%. The threshold of the Q-switched laser operation was found to be approximately 34 mJ, and the output pulse energy at 1064 nm was measured to be 3.5 mJ. The excellent optical-to-optical efficiency of 10.3% affirms this Q-switched Nd:YVO_4 laser to be practical.

In the intracavity OPO experiment, several output couplers with different reflectivities ($34\% \leq R_s \leq 90\%$) at

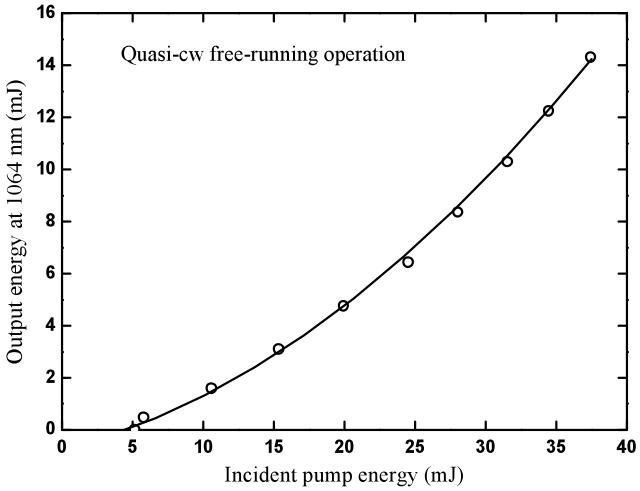

Fig. 4 Output energy at 1064 nm with respect to the incident pump energy at 808 nm for quasi-cw free-running operation

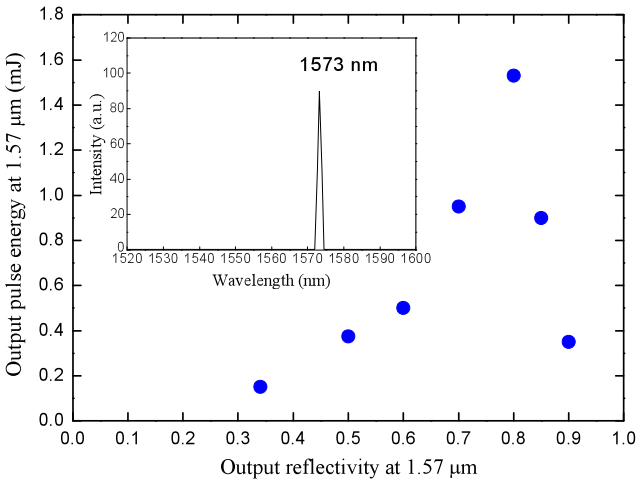

Fig. 5 Experimental results for the output energy at 1573 nm versus the OPO output reflectivity. *Inset*: optical spectrum measurement for the intracavity OPO

1573 nm were used to study the OPO output optimization. Experimental results revealed that the threshold for the OPO output was nearly independent of the output reflectivity R_s and the value was approximately 35 mJ, close to the threshold in the passive Q-switching operation. Figure 5 depicts the experimental results for the OPO output energy versus the OPO output reflectivity. It can be seen that the optimum OPO output reflectivity for the maximum OPO pulse energy is 80%. With the optimum output coupler of $R_s = 80\%$, the single-pulse energy at 1573 nm was up to 1.58 mJ. The spectral information was monitored by an optical spectrum analyzer (Advantest Q8381A) that employs a diffraction grating monochromator to for measure high-speed light pulses with the resolution of 0.1 nm. The optical spectrum measurement is depicted in the inset of Fig. 5.

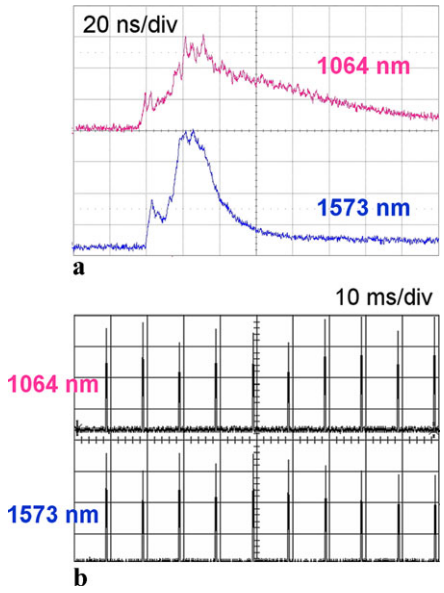

Fig. 6 (**a**) Typical temporal shapes for the fundamental laser and OPO signal pulses. (**b**) An oscilloscope trace of a train of output pulses under a repetition rate of 100 Hz

A LeCroy digital oscilloscope (Wavepro 7100; 10 G samples/sec; 1 GHz bandwidth) with the fast InGaAs photodiodes was used to record the pulse temporal behavior at 1064 nm and 1573 nm. Figure 6(a) shows the temporal shapes of fundamental laser at 1064 nm and the OPO signal at 1573 nm pulses with $R_s = 80\%$. The effective pulse width of the OPO signal can be seen to be approximately 26 ns. By the numerical integration, the OPO peak power was calculated to be approximately 60 kW. Typical oscilloscope trace of a train of the laser and OPO pulses under a repetition rate of 100 Hz is shown in Fig. 6(b). Under the optimum alignment condition, the pulse-to-pulse amplitude fluctuation was found to be less than $\pm 10\%$. The stability of the OPO pulse energy is expected to be improved with actively cooling system for laser diode stack, active medium, and the AlGaInAs saturable absorber. Based on the z-scan technique, the beam quality M^2 factors of the laser beams under free-running, Q-switched, and OPO operations were found to be approximately 4.0, 3.0, and 1.5 respectively. Due to the spatial cleaning effect in the OPO conversion process, beam cleanup was accomplished. The spatial distribution of the OPO signal was recorded with an infrared CCD and displayed in Fig. 7.

5 Summary

In conclusion, we have for the first time employed a AlGaInAs periodic QW saturable absorber to achieve an efficient diode-pumped passively Q-switched Nd:YVO_4 laser

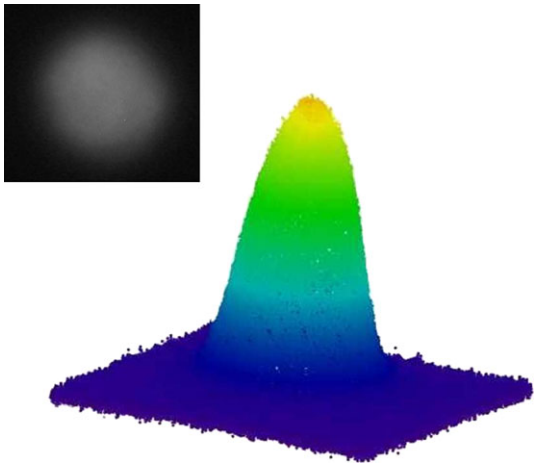

Fig. 7 Experimental transverse pattern of the OPO signal at 1.57 μm

with an intracavity OPO. In a flat-flat resonator with an internal convex lens, we used the optimum output coupler to generate 1.58 mJ signal pulses at 1573 nm at a diode-pumping energy of 35 mJ. The maximum peak power was found to be up to 60 kW. Experimental results reveal that the overall OPO beam quality M^2 factor is better than 1.5 at a pulse repetition rate of 100 Hz.

Acknowledgements The authors gratefully acknowledge various AlGaInAs/InP chips from TrueLight Corporation. The authors also thank the National Science Council for their financial support of this research under Contract No. NSC-97-2112-M-009-016-MY3.

References

1. A. Zavadilová, V. Kubecek, J.C. Diels, Laser Phys. Lett. **4**, 103 (2007)
2. F.Q. Liu, H.R. Xia, Y. Zhong, S.Q. Sun, Z.C. Ling, D.G. Ran, W.L. Gao, J.L. He, H.J. Zhang, J.Y. Wang, Laser Phys. Lett. **5**, 585 (2008)
3. H.Y. Zhu, Y.M. Duan, G. Zhang, C.H. Huang, Y. Wei, W.D. Chen, H.Y. Wang, G. Qiu, Laser Phys. Lett. **7**, 703 (2010)
4. B.T. Zhang, X.L. Dong, J.L. He, H.T. Huang, K.J. Yang, C.H. Zuo, J.L. Xu, S. Zhao, Laser Phys. Lett. **5**, 869 (2008)
5. W. Zendzian, J.K. Jabczynski, J. Kwiatkowski, Appl. Phys. B **76**, 355 (2003)
6. Y.F. Chen, K.W. Su, Y.T. Chang, W.C. Yen, Appl. Opt. **46**, 3597 (2007)
7. Y.P. Huang, H.L. Chang, Y.J. Huang, Y.T. Chang, K.W. Su, W.C. Yen, Y.F. Chen, Opt. Express **17**, 1551 (2009)
8. V. Kubecek, M. Drhokoupil, P. Zatorsky, P. Hirsl, M. Cech, A. Stintz, J.C. Diels, Laser Phys. **19**, 396 (2009)
9. V. Kubecek, M. Jelinek, M. Cech, P. Hirsl, J.C. Diels, Laser Phys. Lett. **7**, 130 (2010)
10. Y.F. Chen, S.W. Chen, Y.C. Chen, Y.P. Lan, S.W. Tsai, Appl. Phys. B **77**, 493 (2003)
11. Y.F. Chen, Y.C. Chen, S.W. Chen, Y.P. Lan, Opt. Commun. **234**, 337 (2004)
12. J. Miao, B. Wang, J. Peng, H. Tan, H. Bian, Appl. Phys. B **88**, 193 (2007)
13. J.G. Miao, B.S. Wang, J.Y. Peng, H.K. Bian, H.M. Tan, Laser Phys. **17**, 1029 (2007)
14. Y.F. Chen, Y.P. Lan, H.L. Chang, IEEE J. Quantum Electron. **37**, 462 (2001)
15. S.C. Huang, S.C. Liu, A. Li, K.W. Su, Y.F. Chen, K.F. Huang, Opt. Lett. **32**, 1480 (2007)
16. Y.P. Huang, P.Y. Chiang, Y.J. Huang, K.W. Su, Y.F. Chen, K.F. Huang, Appl. Phys. B (2010). doi:10.1007/s00340-010-4189-1
17. G. Feugnet, C. Bussac, C. Larat, M. Schwarz, J.P. Pocholle, Opt. Lett. **20**, 157 (1995)
18. R.J. Beach, Appl. Opt. **35**, 2005 (1996)
19. R. Fu, G. Wang, Z. Wang, E. Ba, G. Mu, X. Hu, Appl. Opt. **37**, 4000 (1998)
20. L.M. Frantz, J.S. Nodvik, J. Appl. Phys. **34**, 2346 (1963)
21. B.E. Bouma, J.G. Fujimoto, Opt. Lett. **21**, 134 (1996)
22. B.E. Bouma, M. Ramaswamy-Paye, J.G. Fujimoto, Appl. Phys. B **65**, 213 (1997)